Wave Force Characteristics on a Bottom-pivoted Test Cylinder in the Splash Zone

Nicholas Haritos, Principal Fellow in Infrastructure Engineering, The University of Melbourne
Grattan St., Parkville,Victoria, 3010, E-mail: nharitos@unimelb.edu.au

Abstract

This paper investigates the interaction of a wide variety of gravity waves with a surface piercing bottom pivoted segmented test cylinder in the splash zone in the Morison loading regime from a series of experiments conducted in a wave basin. The splash zone here is defined as the region from the bottom-most trough to the upper-most crest including wave runup on the cylinder concerned. A series of irregular waves conforming to Pierson-Moskowitz wave spectra in uni-directional sea states as well as quasi-regular swept sine waves (SSWs) and another series that considered multi-directional sea states with two different degrees of directional spread were treated in this investigation. Nine abutting segments in the cylinder, of various lengths, were instrumented for in-line and transverse force components. The orthogonal force components in these directions were also measured at the tip supports of the cylinder. A single segment, the longest in the group, was located to ensure capture of the entire splash zone. The orthogonally disposed rigid supports at the top end of the cylinder were also replaced by a set of springs with three different degrees of compliancy to allow dynamic excitation of the test cylinder by the selected wave climates in order to obtain a more comprehensive investigation of the wave-structure interaction in the splash zone and below this zone. Fundamental results obtained suggest that the Morison inertia force coefficients in the splash zone exhibit a frequency dependency and are lower than the corresponding values for the fully wetted segments and for the cylinder as a whole. In addition, the adoption of results for these coefficients from uni-directional waves is conservative for more realistic ocean waves that would exhibit directional spread. Whilst for these tests the drag force was quite small when compared with inertia force in the Morison forcing regime for Keulegan Carpenter numbers less than ~10, it was found that this force component plays a significant role in introducing a hydrodynamic damping contribution to an otherwise very low damping scenario in the case of a compliant cylinder.

Results from these fundamental studies are of particular relevance to designers of offshore structures such as oil rigs/platforms and in the case of bottom-pivoted cylinder designs for tapping renewable energy from ocean wave power.

Keywords: hydrodynamic forcing, Morison force coefficients, hydrodynamic damping

1   INTRODUCTION

The "splash zone" is here defined as the region from the bottom-most trough to the upper-most crest, including wave runup, that the free surface profile of a gravity wave envelopes on any given offshore structural form. In this paper, use of Airy wave theory is made in conjunction with Morison's equation to model for the wave force variation on instrumented segments of a rigid vertical cylinder located in the splash zone and immediately below this zone – ie the fully wetted region and for the cylinder as a whole. Force coefficients in this model are fitted using the method of least squares (for "constant-valued" versions of these coefficients) and, as an alternative, directly obtained from a fit to the Fourier coefficients of the traces concerned (for "frequency-dependent" versions of these coefficients) via experimental measurements obtained from these instrumented segments and at the tip supports, as relevant.

The 0.17m diameter vertical multi-segment surface-piercing test cylinder was tested in 2m depth of water at the wave basin of the National Research Council (NRC) of Canada's hydraulics laboratory in Ottawa, (see Fig. 1). A range of wave inputs was used in these tests which included:

(i)   Repeated Uni-directional Swept Sine Waves (SSW#1 and SSW#2), (Haritos et al., 1989)
(ii)   Uni-directional Pierson-Moskowitz (P-M) waves with frequency at peak wave energy f_p of 0.75, 0.65, 0.6, 0.5, 0.33 Hz at full amplitude
(iii) Three-dimensional sea states conforming to a P-M wave climate with spreading indices of s = 1 (wide) and s = 3 (narrower).
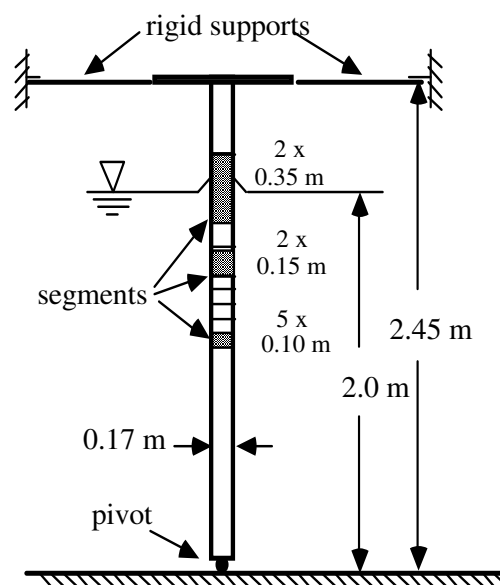

Figure 1 Schematic of Segmented Test Cylinder in NRC Experiments

2.   WAVE KINEMATICS IN THE SPLASH ZONE

The traditional linear wave theory attributed to Airy is generally inadequate for predicting the kinematics of water particles in the splash zone unless it is substantially modified (Sarpkaya and Isaacson, 1981). As an alternative, use can be made of non-linear wave theories (such as Fenton's stream function theory, (Rienecker and Fenton, 1981; Fenton, 1988) to provide more realistic estimates of the associated wave kinematics. Whenever wave amplitudes remain reasonably small (compared to water depth), it has nonetheless been found that Airy wave theory, in its various modified forms of application, can still be an adequate predictor of the water particle kinematics throughout the water depth, inclusive of the splash zone, for both regular and irregular waves, especially for "intermediate" to "deep" water conditions, (Haritos, 1989).

For such Airy waves, the x-directional surface wave profile, $\eta(x,t)$, at position x and at time t for a wave height, H, is given by

$$\eta(x, t) = \frac{H}{2} \cos(\kappa x - \omega t) \tag{1}$$

where $\kappa \, (= 2\pi/\lambda)$ is the wave number, and $\omega \, (= 2\pi/T)$ is the circular frequency with λ and T being the wave length and period respectively and where ω and κ satisfy the traditional form of the dispersion relationship given by

$$\omega^2 = g \, \kappa \, \tanh(\kappa h) \tag{2}$$

in depth of water, h, and for gravitational constant, g.

The alongwave water particle velocity in the x-direction at level z from the Mean Water Level (MWL) at position $x = 0$ for the Airy wave of eqn. (1) is given by $u = u(z,t)$ where

$$u = \frac{\omega H}{2} \frac{\cosh \kappa(z + h)}{\sinh \kappa h} \cos \omega t \tag{3}$$

and the corresponding alongwave water particle acceleration, given by $\dot{u} \, (= \partial u/\partial t) = \dot{u}(z,t)$ becomes

$$\dot{u} = -\frac{\omega^2 H}{2} \frac{\cosh \kappa(z + h)}{\sinh \kappa h} \sin \omega t \tag{4}$$

Chakrabarti (1987) described various "stretch theories" that can be applied to Airy wave theory for prediction of the water particle kinematics in the splash zone. Here, the suggested use of this theory is to apply it in the "normal" way using z values applicable to the splash zone irrespective of the fact that Airy wave theory, strictly speaking, does not hold in this region. (This approach can be labeled as: the "traditional" form of application of Airy wave theory, (Haritos, 1989)).

2.1 Irregular Waves

A uni-directional irregular wave profile, $\eta(t)$, may be considered to be composed of a superposition of Airy wavelets with random phases and amplitudes that would conform to a corresponding wave spectral variation. In the case of an experimentally recorded time series for $\eta(t)$ consisting of N points obtained at a regular time step of dt over a time period of duration of T_d (where $T_d = Ndt$), an expression for $\eta(t)$ can be offered based upon a Fourier series representation, viz

$$\eta(t) = \sum_{n=1}^{N/2} \left(a_n \cos \frac{2\pi nt}{T_d} + b_n \sin \frac{2\pi nt}{T_d} \right) \tag{5}$$

The water particle velocity at location z from the MWL corresponding to this wave profile can be obtained from Airy theory via

$$u(z,t) = \sum_{n=1}^{N/2} A_n \frac{\omega_n \cosh \kappa_n(z+h)}{\sinh \kappa_n h} \cos(\omega_n t - \phi_n) \tag{6}$$

in which circular frequency ω_n $(= 2\pi n/T_d = 2\pi f_n$) and wave number κ_n are related through the dispersion relationship of eqn. (2) and where $A_n = (a_n^2 + b_n^2)^{1/2}$ is the Fourier amplitude of the Airy wavelet at a frequency of $f_n = n/T_d$. The spectrum for $\eta(t)$, viz $S_\eta(f)$, is simply given by

$$S_\eta(f) = \frac{A_n^2}{2} \, T_d \tag{7}$$

Equation (6) can be used to synthesise time series representations for $u(z,t)$ at selected locations, z, from a given recorded time series for the irregular wave profile, $\eta(t)$. Such a synthesis is particularly easy to implement using standard forward/inverse Fast Fourier Transform (FFT) packages that are readily available on a range of computing systems, (Bendat and Piersol, 1986).

The procedure for this synthesis would first require application of the FFT algorithm on the time series for $\eta(t)$ to obtain the (a_n, b_n) or (A_n, ϕ_n) values for each of the $N/2$ Airy wavelets that constitute the wave profile (as in eqn. (5) above). An Inverse FFT is then applied to the wavelet description corresponding to eqn. (6) to obtain the desired time trace for the alongwave water particle velocity at the selected position, z. A similar procedure can then be followed for synthesizing corresponding water particle acceleration traces, $\dot{u}(z,t)$ for irregular waves.

3.   DETERMINATION OF FORCE COEFFICIENTS

Engineers involved with the design of offshore structural forms are concerned about the forcing produced by waves in the splash zone as it is in this region that these forces are considered to attain their peak values for their distribution with depth. Since Morison's equation often forms the basis of the prediction of this wave force distribution, this equation and how it may be applied to a segment of cylinder located in the splash zone becomes of primary interest to the present study.

Morison's equation for the force per unit length, f_R, acting on a rigid surface-piercing cylinder of diameter D is given by

$$f_R = \alpha \dot{u} + \beta u \, | u | \tag{8}$$

where $\alpha = \pi/4 \, \rho \, C_M \, D^2$, $\beta = 1/2 \, \rho \, C_D \, D$ and C_M and C_D are the inertia and drag force coefficients that apply to the cylinder conditions at hand for "rigid" conditions of support.

Several approaches to the determination of the force coefficients, C_M and C_D that apply to a segment of cylinder (whether located in the splash zone or otherwise) can be formulated based upon the Morison expression of eqn. (8) in the situation where experimental records of the time varying in-line force measurements on such a segment in combination with the associated wave profile are available to the study. These may include:

(i)   A treatment based upon a "wave by wave" fitting procedure in the time domain for the case of regular wave or SSW inputs, ($f_1 = 1.25$ to $f_2 = 0.25$ Hz were adopted in this study), (Haritos, 1988; Haritos et al, 1989).

(ii)   A "least squares" spectral fit to this forcing for SSW or irregular wave inputs (Borgman, (1967a)).

(iii) A "frequency-dependent" formulation in these force coefficients based upon a direct fit of the Fourier coefficients of the Morison equation model for the forcing to those obtained from the "observed" force trace.

Conditions (ii) and (iii) above and their implementation for segments that may be either fully submerged or located in the splash zone are described below.

3.1 Coefficients for "Submerged" Segments

For a length of cylinder segment dz located between points z_1 and z_2 where z_1 is below z_2 and z_2 is below the splash zone (hence this segment is always submerged), the in-line force acting on the segment in a rigid support state, $F_X(t)$, can be obtained from

$$F_X(t) = \int_{z_1}^{z_2} f_R \, dz = \int_{z_1}^{z_2} \alpha \dot{u} + \beta u \, |u| \, dz \tag{9}$$

For a random normally distributed u $(= u(z,t))$, the term $u|u|$ in eqn. (9) can be shown to be statistically independent of $\dot{u}$ $(= \dot{u}(z,t))$ by considering a power series expansion for $u|u|$ in terms of u, (Haritos, 1991), hence the spectrum of $F_X(t)$, viz $S_{F_X}(f)$, becomes:

$$S_{F_X}(f) = (\alpha^2 \, S_{F_i}(f) + \beta^2 \, S_{F_d}(f)) \tag{10}$$

where $\quad F_i(t) = \int_{z_1}^{z_2} \dot{u} \, dz = \sum_{n=0}^{N/2} g \, \frac{sinh\kappa(h+z_2) - sinh\kappa(h+z_1)}{cosh\kappa h} \eta_{\pi/2}$ $\tag{11}$

in which $\eta_{\pi/2}$ is the version of the Airy wavelet obtained from the wave profile at frequency $f = n/T_d$ that lags this wave by a phase of $\pi/2$, and

$$F_d(t) = \int_{z_1}^{z_2} u \, |u| \, dz \tag{12}$$

$F_i(t)$ is interpreted as the inertia force trace for a unit value of α whilst $F_d(t)$ corresponds to the drag force trace for a unit value of β for the segment concerned.

The spectrum for $F_i(t)$ viz $S_{F_i}(f)$, can be obtained from eqn. (11) as:

$$S_{F_i}(f) = (\, g \, \frac{sinh \, \kappa(h+z_2) - sinh \, \kappa(h+z_1)}{cosh \, \kappa h} \,)^2 \, S_\eta(f) \tag{13}$$

The spectrum for $F_d(t)$, viz $S_{F_d}(f)$, can be obtained from a step-by-step procedure that may be summarised as follows:

1. For a given $\eta(t)$ obtain the Fourier coefficients (a_n, b_n) via an FFT (see eqn. (5)).
2. Choose equal subdivisions of the segment with a spacing $(z_2 - z_1)/M$ and $M+1$ an odd number of positions to evaluate $u(z_i, t)$ via the inverse FFT procedure described in 2.1 above.
3. Obtain $u_i|u_i|$ from simulated traces of $u(z_i, t)$ obtained at all $M+1$ positions on the segment.
4. Use Simpson's rule to obtain a numerical integration "equivalent" for $F_d(t)$ from eqn. (12).
5. Use an FFT on the resultant $F_d(t)$ to obtain the corresponding Fourier coefficients. Hence obtain the spectrum from its relationship to the Fourier amplitudes via a version of eqn. (7) as it would apply to the formation of $S_{F_d}(f)$ instead.

3.1.1 "Constant-valued" force coefficients

With spectra for $F_i(t)$ and $F_d(t)$ now determined via the techniques described above, the predicted form of $S_{FX}(f)$ can be obtained for any nominated (C_M, C_D) combination. This prediction can then be compared with the observed form of this spectrum for the corresponding segment force as obtained from direct measurements in the wave tank experiments.

It is also possible using the standard approach of the method of least squares to optimize for the values of α^2 and β^2 that "best" fit the form of force spectrum, $S_{FX}(f)$, predicted via eqn. (10), to that obtained directly from experimental measurements of the force trace, $F_X(t)$. (Details of the implementation of the method are given by Borgman, (1967a)). Hence the optimal "constant-valued" forms of C_M and C_D can be inferred directly from the definitions of α and β, using values of the latter obtained via this "least squares" approach.

3.1.2 "Frequency-dependent" force coefficients

As an alternative to the traditional "constant-valued" force coefficient formulation of the Morison equation given by eqn. (8), the C_M and C_D combination can instead be considered to be "frequency-dependent" viz $C_M(f)$, $C_D(f)$ respectively. Values for $C_M(f)$, $C_D(f)$ for a fully submerged segment can be estimated from an exact fit to the Fourier coefficients obtained from the measured form of $F_X(t)$ and those from the prediction via eqn. (9) in which "frequency-dependent" versions of the force coefficients have been adopted in eqn. (8) for $f_R(z,t)$ instead of "fixed values". The FFT method can be used on each respective time trace concerned to establish the corresponding pair of Fourier coefficients (a_n, b_n) that apply at regular frequency ordinates of $f = n/T$. The "fit" is then conducted on the resultant Fourier coefficients, viz

$$(a_n, b_n)_{FX} = \alpha(f) (a_n, b_n)_{F_i} + \beta(f) (a_n, b_n)_{F_d} \tag{14}$$

where $\alpha(f) = \frac{\pi}{4} \rho C_M(f) D^2$ and $\beta(f) = \frac{1}{2} \rho C_D(f) D$.

Equation (14) produces a pair of simultaneous linear equations at each frequency increment that can be solved to obtain the "local values" of $\alpha(f)$ and $\beta(f)$ and hence the $(C_M(f), C_D(f))$ combination that applies to the segment under consideration.

3.2 Coefficients in the Splash Zone

The evaluation of the force coefficients in the splash zone follows along similar lines to the descriptions above for the case of a fully submerged segment except that the integrations involved need now be performed over the "wetted" portion of this segment at any instant.

Equation (9) therefore needs be expressed as

$$F_X(t) = \int_{z_1}^{\eta(t)} f_R \, dz = \int_{z_1}^{\eta(t)} \alpha \dot{u} + \beta u |u| \, dz \tag{15}$$

where $F_i(t)$ and $F_d(t)$ now become $F_i(t) = \int_{z_1}^{\eta(t)} \dot{u} \, dz$ and $F_d(t) = \int_{z_1}^{\eta(t)} u |u| \, dz$

The procedure adopted here to evaluate these two integrals is to subdivide the splash zone segment into a number of equal length portions where the top edge of portion j is located at level z_j. Closed form solutions to $F_i(t)_j$ and numerical solutions to $F_d(t)_j$ (that have been obtained in the manner of the "fully submerged" segment situation) that would correspond to the case of this segment being wetted from z_1 to z_j then follow. This set of traces for each of these force contributions, once obtained in this way, can then be interpolated at any instant in time to obtain the result that would now correspond to the wetted position, $\eta(t)$.

This procedure can then be implemented to obtain either "constant-valued" or "frequency-dependent" force coefficients respectively for a segment located in the splash zone via similar approaches to those outlined above for the case of a submerged segment.

4.   DESCRIPTION OF THE EXPERIMENTS

As well as the force measurements at the supports and the orthogonal force components for each segment, measurements were also conducted of wave height at two separate locations: one alongside the cylinder and the other at its adjacent "point of symmetry" in the NRC wave basin. Data sampling was conducted digitally at the rate of 10 Hz over 819.2 seconds to produce 8192 points for each channel. Wave generation was via a 60 paddle random-wave generator capable of producing both uni-directional and multi-directional sea states with pre-specified characteristics: a "state of the art" facility. The data acquisition and wave generation equipment were both controlled by a Hewlett-Packard 1000F minicomputer on which data files for all records were intermediately stored prior to transfer to a micro-VAX cluster for subsequent analysis, (Haritos, 1991).

5.   OBSERVED VARIATIONS FOR FORCE COEFFICIENTS

The NRC test cylinder was found to be inertia force dominant for all test conditions in these experiments. Data was not well conditioned for the determination of C_D values so that reliable fits were conducted for C_M and $C_M(f)$ variations only. (It should be noted here that although drag force is rather small and C_D values were not able to be determined, this force mechanism is important towards enabling a hydrodynamic damping contribution for when the cylinder is compliant).

Figures 2 and 3 summarize the results for the constant-valued C_M coefficients obtained for the splash zone segment and fully-wetted segment immediately below it and compares these results with the values obtained for the cylinder "as a whole", over the range of Pierson Moskowitz waves adopted in these tests. It is clear that the C_M values observed on the splash zone segment are significantly smaller than those obtained for the segment below and for the cylinder "as a whole" suggesting that wave forcing in the splash zone may not be as severe as may be "feared" by offshore structure designers. In addition, there appears not to be a significant dependence on Keulegan Carpenter number in the inertia force dominant region of KC < 8 of the C_M coefficient nor a dependence of it on spreading index, inferring that uni-directional tests in a wave tank (as opposed to a more expensive wave basin facility) would be sufficient for inertia dominant conditions.

Figure 4(a) and (b) depicts the frequency dependence of the C_M values for the segment in the splash zone and that for the fully wetted segment. Results show that whilst the $C_M(f)$ values for the splash zone segment for very low wave frequencies are similar to those for the fully wetted segment, these values do show a frequency dependence that reduces the value with frequency whereas this reduction with frequency is not seen for the fully wetted segment. There also appears not to be a significant influence of wave type: quasi-regular SSW's or different P-M waves that are uni-directional ($s = \infty$ but here taken as 10) or waves with energy spread (P-M waves with $f_p = 0.5$ Hz and spreading indices of $s = 1$ or 3). This would suggest that a constant value of 2.0 (the theoretical value for inertia dominant cylinders) can be reasonably adopted for this spread of wave conditions.
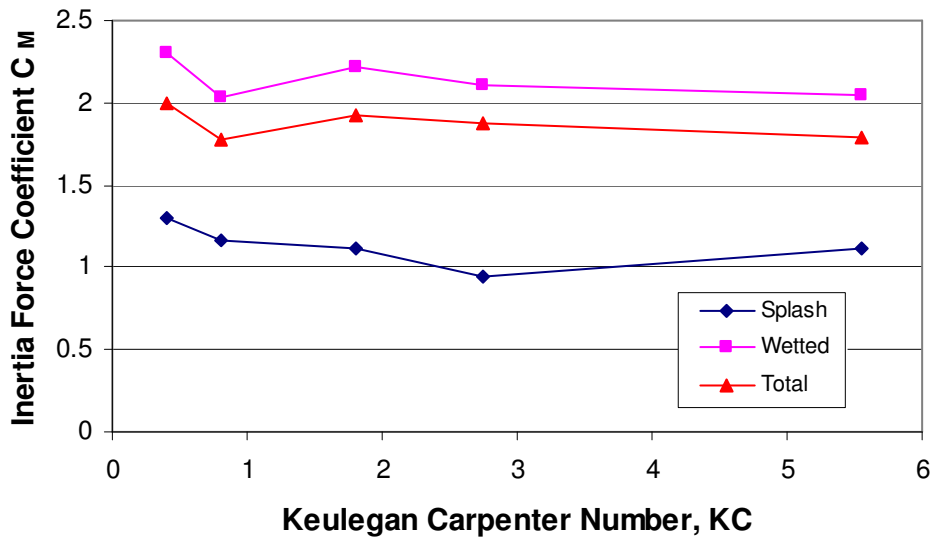
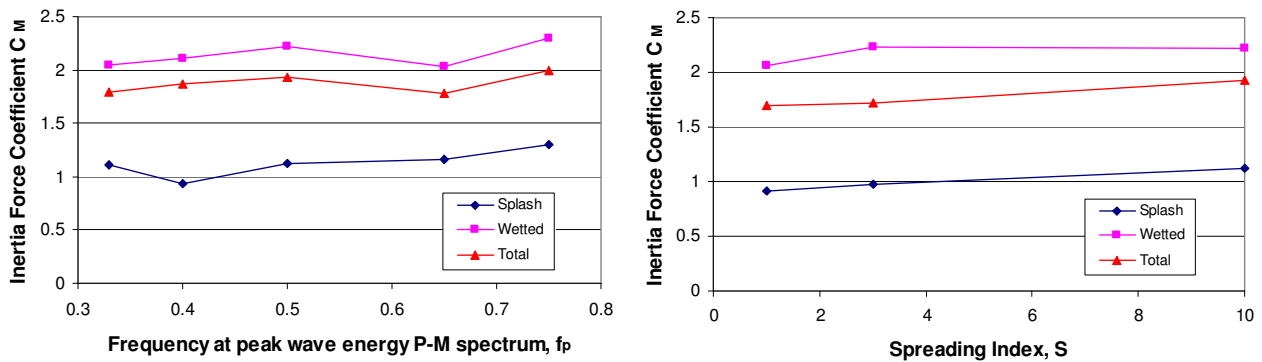Figure 2: Variation of C_M with Keulegan Carpenter number, KC

Figure 3: Variation of C_M with frequency at peak wave energy, f_p, and spreading index S
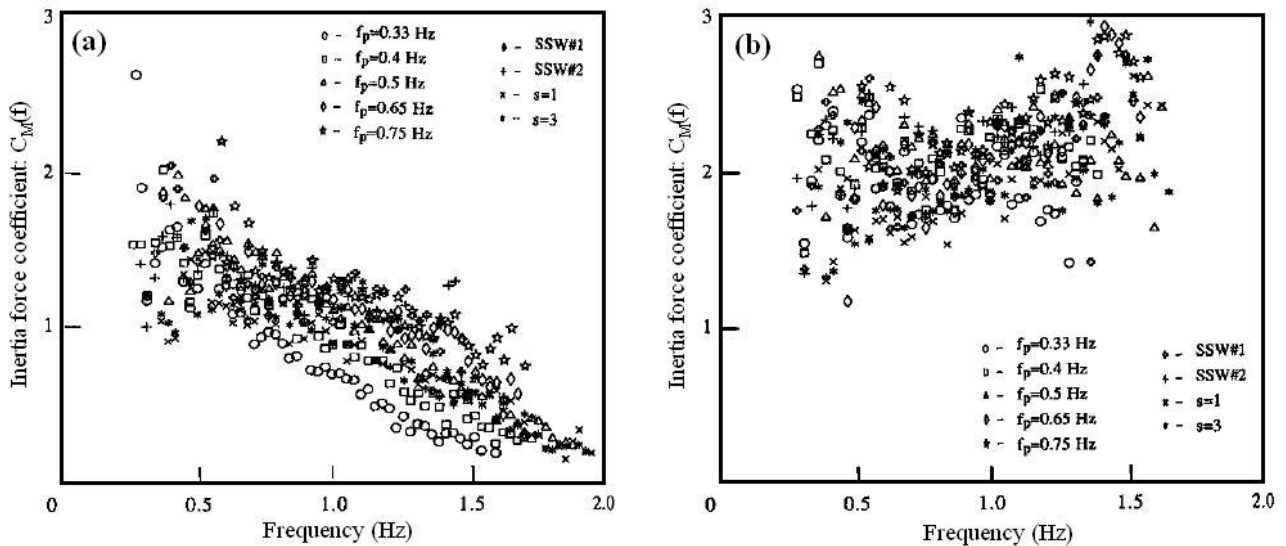

Figure 4: Variation of $C_M(f)$ with frequency for (a) splash zone and (b) fully wetted segment

6.   CONCLUDING REMARKS

Experiments have been performed on a segmented vertical surface-piercing cylinder with instrumented segments located in the splash zone and separately immediately below this position.

These have provided estimates of both "constant-valued" and "frequency-dependent" versions of the Morison inertia force coefficient C_M for a range of wave climates.

Characteristics of C_M obtained for the splash zone can be summarised as follows:

    (i) Values for C_M appear to be generally lower than those observed for the "wetted" segments and for the cylinder "as a whole", for all the wave types tested, allaying the fears of would be designers of offshore structures for possibly highly extreme loading conditions in this region.

  (ii) There is a slight frequency-dependence in the values of $C_M(f)$ for the splash zone whereas this dependence is not observed for the "fully wetted" regions of the cylinder.

7.   ACKNOWLEDGEMENTS

8.   REFERENCES

Bendat, J.S and Piersol, A.G., (1986), Decomposition of Wave Forces into Linear and Non-linear components, *Jl. of Sound and Vibration*, Vol 106, No. 3, pp 391-408.

Borgman, L.E., (1967a), Spectral Analysis of Ocean Wave Forces on Piling, *Proc. ASCE Jl. Waterways & Harbors Division*, Vol. 93, No. WW2, pp 129-156.

Borgman, L.E., (1967b), Random Hydrodynamic Forces on Objects, *Annals of Mathematical Statistics*, Vol. 38, pp 35-51.

Chakrabarti, S.K., (1987), *Hydrodynamics of Offshore Structures,* Computational Mechanics Publications.

Fenton, J.D., (1988), The Numerical Solution of Steady Water Wave Problems, *Computers & Geoscience,* Vol. 14, No.3, pp 357-368.

Haritos, N., (1988), *The Swept Sine Wave Technique in Hydrodynamic Applications,* Dept. of Civil & Agric. Engineering, University of Melbourne Tech. Report, TR/Struct/01/88.

Haritos, N., (1989), "Hydrodynamic Damping of Compliant Vertical Cylinders in Waves", *Proc. SSA-IMACS Conf.,* Canberra, Australia, pp 214-219.

Haritos, N. (1991), Hydrodynamic Force Coefficients in the Splash Zone, *Proc. 1ˢᵗ ISOPE Conference*, Edinburgh, UK, 11-16ᵗʰ August, pp194-202.

Haritos, N., Cornett, A.M. and Nwogu, O., (1989), The Swept Sine Wave - An Invaluable Tool for Hydrodynamic Research, *Proc. XIII Congress IAHR,* Ottawa, pp C485-C492.

Rienecker, M.M. and Fenton, J.D., (1981), A Fourier Approximation Method for Steady Water Waves, *Jl. Fluid Mechanics,* Vol. 104, pp 119-137.

Sarpkaya, T. and Isaacson, M., (1981), *Mechanics of Wave Forces on Offshore Structures,* Van Nostrand Reinhold, N.Y.